PHYSICAL REVIEW E **72**, 030201(R) (2005)

Internal fluid dynamics in levitated drops by fast magnetic resonance velocimetry

A. Amar, S. Stapf, and B. Blümich
Lehrstuhl für Makromolekulare Chemie, ITMC, RWTH Aachen, Worringerweg 1, D-52074 Aachen, Germany
(Received 16 March 2005; published 13 September 2005)

Fluid motion inside a levitated drop is determined by the interface properties. Momentum transfer through a highly mobile interface results in stationary vortex patterns inside the drop that dramatically enhance mass transfer between both phases, while immobile interfaces suppress internal dynamics. The presence of small amounts of surface-active substances can result in a partial reduction of interface mobility, the so-called rigid cap. The time dependence of internal flow patterns is presented by means of NMR velocity images of levitated drops, and is compared to fast measurements of the velocity distribution along the three orthogonal coordinates.

DOI: 10.1103/PhysRevE.72.030201 PACS number(s): 47.32.−y, 68.05.−n, 82.56.−b, 83.50.−v

Liquid-liquid extraction processes are of widespread use in chemical engineering and have their most important application in separation procedures where contaminants in a bulk, valuable fluid component (donator phase) are removed by bringing them into contact with a second, disperse phase (acceptor phase). In order to provide maximum transfer within a given amount of time, a large interface area between the two main phases is desired. This is often realized by dispersing the acceptor phase into a swarm of droplets and allowing it to pass through the continuous phase, exploiting the density difference. It is a well-known fact [1–3] that the efficiency of mass transfer between the two phases is determined by convective transport made possible through circulation occurring both inside and outside the droplets. Modeling mass transfer, however, depends on a precise knowledge of the fluid dynamics inside the drop, the only experimental evidence usually being delivered from integral measurements of the mass transfer in an extraction column. While particle-tracer techniques have been used to qualitatively visualize the flow field in drops [3–6], they remain limited in delivering quantitative information about the velocity field. Moreover, they are invasive and can potentially affect the delicate balance between fluid hydrodynamics and interface-active species that reduce the drop mobility. Nuclear magnetic resonance (NMR) velocity imaging is noninvasive and can give quantitative information about drop shape and velocities and is able to distinguish between different chemical compounds that will become relevant for the direct investigation of mass transfer.

NMR imaging applications to transport phenomena are currently gaining increased acceptance in various fields related to engineering problems [7,8]. Often, transport through model reactors is investigated where rather coarse spatial resolutions are sufficient, while NMR microscopy [9] was used to understand flow processes even on sub-millimeter scales [10–14]. In [15], velocity imaging inside a falling water drop has been demonstrated as a feasibility study to resolve velocity patterns in a small and fast moving object, requiring typical experimental times of many hours. In a preparatory study, the internal dynamics of single silicone oil drops was found to be time invariant but extremely slow due to the almost rigid drop interface [16]. The monitoring of complex dynamics on a small scale, particularly under (on time scales between seconds to hours) non stationary conditions, requires velocity imaging strategies that combine high spatial and temporal resolution with the potential to distinguish the distribution of different chemical species.

In this paper, fast NMR imaging techniques are combined with velocity encoding in order to generate statistical and imaging information about the internal drop dynamics. Single levitated drops made from toluene (99.5 purity, Aldrich) balanced in a counterstream of the continuous phase, D_2O (99.8% deuteration, Aldrich), are investigated. The levitated drops were held in place in the narrowing section of a glass pipe as shown schematically in Fig. 1. The cell and periphery was designed and constructed at the Department of Chemical Engineering-Thermal Unit Operations (TVT), RWTH Aachen; a design optimization routine was employed that is described in [17]. The cell of a total length of 170 cm was mounted vertically inside the bore of a superconducting NMR magnet and filled with D_2O, which was continuously pumped from top to bottom. A drop was released from a dosimeter at the bottom end of the cell and rose up due to its lower density; the position of force balance under the influence of the increased flow velocities of the continuous phase in the narrowing part of the cell coincided with the center of the NMR resonator. The rise time of the drop to reach this

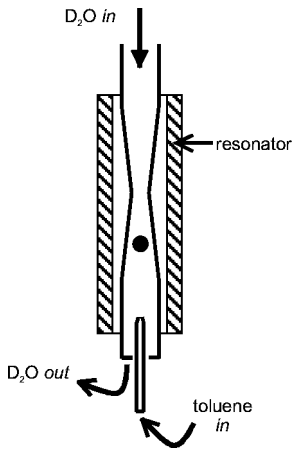

FIG. 1. Schematic drawing of the glass cell holding the levitated drop.

position was 20 s. Bruker Micro 2.5 microimaging gradient sets and probes were used, and experiments were carried out on a Bruker DSX 500 spectrometer. Data analysis was performed using PROSPA software (Magritek, Wellington, New Zealand).

The image and velocity information in an NMR experiment both rely on the same principle of spatially dependent magnetic field strengths provided by pulsed field gradients (PFGs). The Larmor frequency ω can generally be written as

$$\omega(\mathbf{r}) = |\gamma(\mathbf{B_0} + \mathbf{gr})|, \tag{1}$$

where γ is the gyromagnetic ratio of the proton ($\gamma = 2.6752 \times 10^8$ $\mathrm{T^{-1}\,s^{-1}}$), $\mathbf{g}$ is the first derivative of the z component of the magnetic field strength $\mathbf{B}$ with respect to space, and $\mathbf{B_0}$ is the constant main field. This provides one possibility to generate image information by acquiring the signal in the presence of a gradient so that the Fourier transform of the signal corresponds to the one-dimensional projection of the object onto the gradient axis, assuming that the intrinsic Larmor frequency in the constant field, $\omega_0 = |\gamma(\mathbf{B_0})|$, is identical for all spins. The second approach exploits the phase information, which is acquired with the complex NMR signal. Applying a *pulsed* gradient $\mathbf{g_{phase}}$ for a duration δ generates a phase shift

$$\varphi(\mathbf{r}) = (\omega(\mathbf{r}) - \omega_0)\,\delta = 2\pi\mathbf{kr} \tag{2}$$

relative to a reference value, where the wave vector is defined as $\mathbf{k} = (2\pi)^{-1}\gamma\mathbf{g_{phase}}\delta$. The total signal intensity $\tilde{S}(\mathbf{k})$—normalized by its value in the absence of a gradient—can then be written as an integral over all spins in the sample,

$$\tilde{S}(\mathbf{k}) = \int P(\mathbf{r})\exp[i2\pi\mathbf{kr}]d\mathbf{r}. \tag{3}$$

Scanning k space evenly allows the reconstruction of the spin-density function $P(\mathbf{r})$ following an inverse Fourier transformation. The scheme can be combined to obtain three-dimensional images, and a wide range of techniques have been developed that reduce the acquisition time of a full image considerably by either repeated refocusing of the signal or sectioning of the magnetization.

Velocity v, or rather displacement $\mathbf{R}$ during an interval Δ, is encoded in much the same way, by applying a pair of gradient pulses of opposite sign but identical area. This gradient pulse pair gives rise to a phase shift $\varphi(\mathbf{R}) = 2\pi\mathbf{kR}$ that is proportional to displacement and can be used for individual encoding schemes as well as in combination with the mentioned imaging sequences. In analogy to phase encoded imaging, the distribution function of velocities, $P(\mathbf{v})$, can be reconstructed.

In order to verify the positional stability of the drops, series of one-dimensional frequency encoded profiles with separations of 200 ms were acquired over times of several minutes. The drops were found to remain at the same position with an error limit that was below the spatial resolution of the technique of 20 μm. The drops were oblate with vertical and horizontal diameters of 3.6 and 4.3 mm, respectively. The two-line NMR spectrum of toluene required the selective excitation of one of the resonance lines by using a narrow-band radio frequency pulse to avoid blurring of the image. This technique, which allowed the suppression of between 95% and 99% of the unwanted remaining signal contributions, will eventually be used for separating different proton-containing compounds in a multicomponent system.

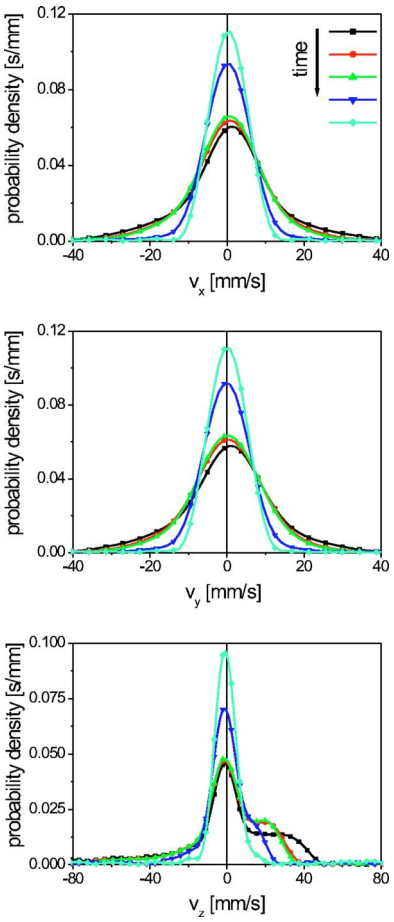

FIG. 2. (Color online) Probability densities of velocities in the toluene drop; all three orthogonal components of the velocity are plotted separately. Times indicating the drop age, beginning with the separation of the drop from the pipette, are as follows (see symbols from top to bottom): 5 min, 49 min, 90 min, 120 min, 11 h.

In Fig. 2, the velocity distributions in toluene drops are shown for motion in horizontal (x,y) and vertical (z) directions. The data acquisition for velocities in one direction took 32 s. The distributions represent weighted averages over the total volume of the drop. The velocity of the continuous phase at the location of the drop was about 160 mm/s; the maximum velocities found inside the drop are considerably lower but still of the same order of magnitude. This is in contrast to the findings for silicone oil drops floating in water [16] where only minor internal circulation (1–2 mm/s) were observed due to the almost rigid interface. Water-toluene represents an established standard test system for extraction analysis, and a mobile interface is expected for toluene drops of this size, which is supported by findings from sedimentation experiments. It is therefore not surprising that considerable momentum transfer takes place across the interface into

the drop interior, and large internal velocities do occur.

The maximum values and the shape of the velocity distribution functions vary noticeably with time. This confirms a common observation that under experimental conditions where surface-active impurities are present, the drop dynamics is being reduced with time and the drop is slowly "dying." In the presented experiments, heavy water (D_2O) was first saturated with toluene by shaking a container containing both fluids and subsequent separation of the liquids. No attempt was made to further enhance the amount of organic impurities. The contaminants present in the system were sufficient to promote a slow and gradual change of the drop dynamics over periods of several hours as is demonstrated in Fig. 2. The distributions of the transverse components, v_x and v_y, which remain similar to each other and symmetric throughout the experiment, experience a reduction of the maximum velocity values from about 40 mm/s at the first measurement to about 15 mm/s after a time of eleven hours. This behavior was observed repeatedly but with different time dependence, which can be attributed to the varying concentration of impurities in the system. The velocity distributions plotted for 11 hours correspond approximately to an equilibrium situation, i.e., no noticeable changes were found for longer times, and repeated experiments led to very similar spreads of velocities in the long-time limit. Note that an asymmetry is retained for v_z (vertical component) even for the longest times, while the probability distribution of v_x and v_y is generally symmetric.

The presented method of fast velocity distribution analysis is suitable for providing general information about the drop dynamics, in particular about its evolution with time in the first minutes after settling. However, it is insufficient for quantifying the internal velocity fields and to provide data for a validation or falsification of existing fluid dynamics models. This has to be achieved by combining NMR imaging with a velocity encoding module, a method that enhances information content at the cost of experimental time.

Integral velocity images (projections onto a vertical plane) are shown in Fig. 3 for the toluene drop; the acquisition time for each image was 7 min. Because of the relatively large velocities occurring in toluene, a multiecho technique that speeds up signal acquisition could not be used, as the motion of the spins during repeated acquisitions would potentially exceed the pixel size significantly. Instead, one image encoding step had to be taken for each velocity encoding, and repetition required a time delay of 200 ms to achieve partial recovery of the magnetization. Integral velocity images could be acquired in 14 min. Figure 3 (top) shows a pronounced vortex pattern in the upper half, but hardly any motion in the lower half of the drop. This behavior is fully understood and described in [4,18–20] as being the consequence of an incomplete interface mobility due to impurities or agents affecting the interface tension. It appears at the downstream side of the drop that coincides with the drop's bottom half in this study, as the flow direction of the continuous phase is from top to bottom. The "rigid cap" is expected to grow with time if more impurities aggregate at the interface. Indeed, Fig. 3 clearly demonstrates not only the growth of the cap with increasing time, but also the decrease of velocity magnitudes in the upper part of the drop. This

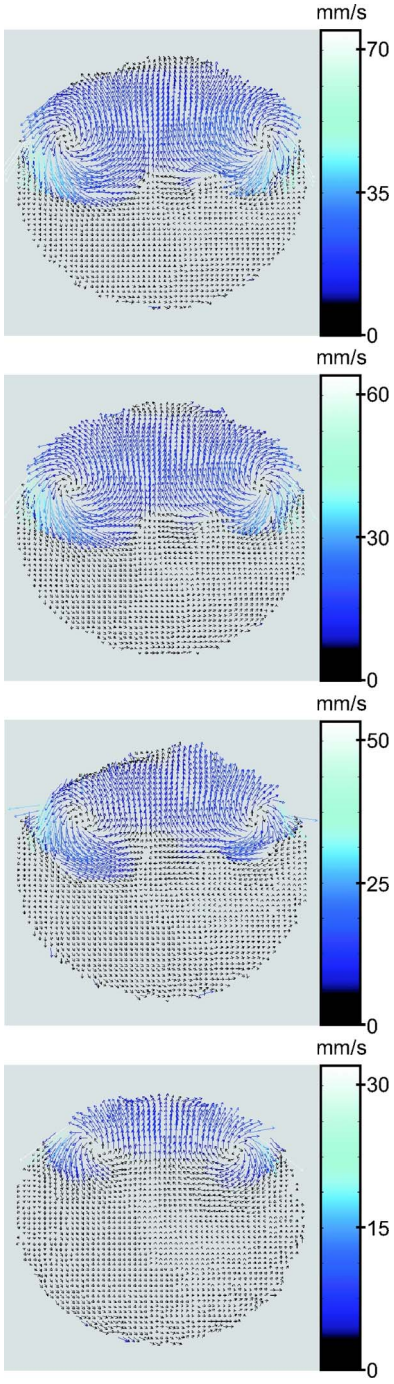

FIG. 3. (Color online) Vector plots of the internal velocities in a toluene drop as a projection onto a vertical plane. Times indicating the drop age, beginning with the separation of the drop from the pipette, are as follows (from top to bottom): 7, 51, 92, 122 min.

series corresponds to the propagator measurements of Fig. 2, and experiments were carried out alternately so that each velocity image was preceded by a comparable set of propagator measurements along the three spatial directions. The range of velocities found in the images is in good agreement with the results of propagator measurements (note that the arrow length corresponds to the speed, $\sqrt{v_y^2+v_z^2}$, while Fig. 2 presents the components v_x, v_y, v_z individually). The highest velocities can be attributed to a relatively small fluid volume

in the vicinity of the vortices. They are partially covered in the propagator plots of v_z where they appear as a small and broad probability density at negative values. A certain averaging effect in the propagators is possible due to the different velocity encoding times($\Delta=10$ ms for propagators, $\Delta=5$ ms for images): during a longer encoding time, spins are more likely to change their velocities, hence the maximum observed value becomes lower for growing Δ.

The more time-consuming velocity imaging experiments reveal the true nature of the change of internal motion, while the faster propagator measurements provide an indirect measure of the internal mobility that is, nevertheless, sufficient for monitoring the mobility of the drop as a whole, a critical parameter for verifying whether optimal mass transfer in such a system takes place and to what degree it is compromised by impurities that limit the lifetime of the drop as an efficient extraction site.

In conclusion, the feasibility of applying PFG-NMR techniques for the noninvasive investigation of internal fluid dynamics in levitated drops was demonstrated. The technique is both reasonably fast and allows the visualization of three-dimensional velocity fields for providing input data to interface models and to allow a comparison with numerical simulations that are currently under way. While invasive methods can provide part of the motion information, they are inferior with respect to temporal and spatial resolution and might potentially affect the very subject of interest, the fluid dynamics itself. The application of spectrally selective techniques to generate images from a species containing a multiline spectrum (toluene) suggests the next logical step of employing NMR velocity imaging as a means to monitor mass transfer and eventually reactions inside single drops, and to quantify the different compounds involved. The high stability and favorable geometry of this experimental setup bear the potential of developing it into a routine experimental chamber with application fields as manifold as reactive extraction and emulsion polymerization. A better understanding of the dependence of hydrodynamics near interfaces and its dependence on surface-active compounds, and a means to directly monitor these processes, is of vital importance for a large class of processes where immiscible fluids are in contact with each other and subject to momentum as well as mass transfer.

This work has been supported by DFG within the Collaborative Research Centre (SFB) 540 at RWTH Aachen. We are grateful to E. Groß-Hardt for continuing support in constructing and improving the experimental setup, and to E. Groß-Hardt and A. Pfennig for discussions of the experimental results. L. Buljubasich, M. Küppers, M. Voda, and A.A. Khrapitchev are acknowledged for their invaluable contributions to this project.

[1] R. Clift, J. R. Grace, and M. E. Weber, *Bubbles, Drops and Particles* (Academic Press, New York, 1978).
[2] *Recent Advances in Liquid-Liquid Extraction*, edited by C. Hanson (Pergamon, Oxford, 1971).
[3] J. T. Davies, *Turbulence Phenomena* (Academic Press, New York, 1972).
[4] P. Savic, Nat. Res. Counc. Can. Report No. MT-22, 1953.
[5] S. K. Chung and E. H. Trinh, Phys. Fluids **12**, 249 (2000).
[6] T. Uemura and M. Yamauchi, KSME Int. J. **15**, 1845 (2001).
[7] E. Fukushima, Annu. Rev. Fluid Mech. **31**, 95 (1999).
[8] L. F. Gladden, AIChE J. **49**, 2 (2003).
[9] P. T. Callaghan, *Principles of Nuclear Magnetic Resonance Microscopy* (Clarendon Press, Oxford, 1991).
[10] A. J. Sederman, M. L. Johns, P. Alexander, and L. F. Gladden, Chem. Eng. Sci. **53**, 2117 (1998).
[11] U. Tallarek, E. Bayer, D. van Dusschoten, T. Scheenen, H. Van As, G. Guiochon, and U. D. Neue, AIChE J. **44**, 1962 (1998).
[12] M. M. Britton and P. T. Callaghan, Eur. Phys. J. B **7**, 237 (1999).
[13] M. Weber and R. Kimmich, Phys. Rev. E **66**, 056301 (2002).
[14] X. Ren, S. Stapf, and B. Blümich, AIChE J. **51**, 392 (2005).
[15] Song-I. Han, S. Stapf, and B. Blümich, Phys. Rev. Lett. **87**, 144501 (2001).
[16] A. Amar, E. Gross-Hardt, A. A. Khrapitchev, S. Stapf, A. Pfennig, and B. Blümich J. Magn. Reson. **177**, 76 (2005).
[17] E. Gross-Hardt, E. Slusanschi, H. M. Bücker, A. Pfennig, and C. H. Bischof (unpublished).
[18] F. H. Garner and A. H. P. Skelland, Chem. Eng. Sci. **4**, 149 (1955).
[19] R. H. Magarvey and J. Kalejs, Nature (London) **198**, 377 (1963).
[20] G. C. Quintana, Int. J. Heat Mass Transfer **33**, 2631 (1990).